

Dissipative soliton operation in a mode-locked laser based on thulium-doped fiber

Wen-Yan Zhang(张文艳), Lei Zheng(郑磊), Tian Zhang(张添), Nan-Nan Liu(刘楠楠), Li-Jie Geng(耿利杰), Kun Yang(杨坤), and Li Zhan(詹黎)

Citation: Chin. Phys. B, 2026, 35 (**4**): 044201. DOI: 10.1088/1674-1056/ae063c
http://cpb.iphy.ac.cn; http://iopscience.iop.org/cpb

What follows is a list of articles you may be interested in

High-efficiency Yb^{3+}-doped fiber laser with highly optical nonlinear Bi_4Br_4-based saturable absorber

Mengyuan Liu(刘梦媛), Yechao Han(韩烨超), Qi Liu(刘齐), Hao Teng(滕浩), Xiwei Huang(黄玺玮), Xiaowei Xing(邢笑伟), Xiangyu Qiao(乔向宇), Guojing Hu(胡国静), Xiao Lin(林晓), Haitao Yang(杨海涛), Zhiyi Wei(魏志义), and Wenjun Liu(刘文军)
Chin. Phys. B, 2025, 34 (**6**): 064202. DOI: 10.1088/1674-1056/adc664

Pure-quartic soliton molecules in normal fourth-order dispersion regimes based on spectral filtering effect

Han-Yang Shen(申翰阳), Rui-Bo Lan(蓝睿博), Hong-Bin Hu(胡洪彬), Yang Li(李阳), Rui Zhou(周瑞), and Zu-Xing Zhang(张祖兴)
Chin. Phys. B, 2025, 34 (**3**): 034203. DOI: 10.1088/1674-1056/ada43c

Dissipative soliton resonance within different dispersion regimes in a single mode-locked laser

Zhetao Zhao(赵哲韬), Qinke Shu(舒沁珂), Ziyi Xie(解梓怡), Yuxuan Ren(任俞宣), Ying Zhang(张颖), Bo Yuan(袁博), Chunbo Zhao(赵春勃), Junsong Peng(彭俊松), and Heping Zeng(曾和平)
Chin. Phys. B, 2024, 33 (**7**): 074208. DOI: 10.1088/1674-1056/ad47b1

On the generation of high-quality Nyquist pulses in mode-locked fiber lasers

Yuxuan Ren(任俞宣), Jinman Ge(葛锦蔓), Xiaojun Li(李小军), Junsong Peng(彭俊松), and Heping Zeng(曾和平)
Chin. Phys. B, 2024, 33 (**3**): 034210. DOI: 10.1088/1674-1056/acfa87

Wavelength switchable mode-locked fiber laser with a few-mode fiber filter

Shaokang Bai(白少康), Yujin Xiang(向昱锦), and Zuxing Zhang(张祖兴)
Chin. Phys. B, 2023, 32 (**2**): 024209. DOI: 10.1088/1674-1056/ac744f

---

Dissipative soliton operation in a mode-locked laser based on thulium-doped fiber

Wen-Yan Zhang(张文艳)[1], Lei Zheng(郑磊)[1], Tian Zhang(张添)[1], Nan-Nan Liu(刘楠楠)[1], Li-Jie Geng(耿利杰)[1], Kun Yang(杨坤)[1,†], and Li Zhan(詹黎)[2]

[1] *School of Electronics and Information, Zhengzhou University of Light Industry, Zhengzhou* 450002, *China*
[2] *State Key Laboratory of Advanced Optical Communication Systems and Networks, School of Physics and Astronomy, Shanghai Jiao Tong University, Shanghai* 200240, *China*

(Received 16 July 2025; revised manuscript received 28 August 2025; accepted manuscript online 12 September 2025)

We report a dissipative soliton laser utilizing thulium-doped fiber as the saturable absorber. By adjusting the polarization controller and pump power, a stable fundamental dissipative pulse has been successfully achieved, featuring a center wavelength of 1565.88 nm, a 3-dB bandwidth of 1.20 nm, a repetition frequency of 36.9 MHz, and a signal-to-noise ratio of 64 dB. Combined the gradual increase of the pump power with the intracavity polarization optimization, the spectral morphology evolves into a parabolic shape, Π-shape, and M-shape. Moreover, through increasing the gain, multiple dissipative pulses include dissipative soliton pairs and triples are manifested because of the peak power clamping effect. The repetition frequencies are 73.8 MHz and 110.7 MHz, respectively, with signal-to-noise ratios both more than 60 dB, indicating that the constructed dissipative soliton laser has excellent stability. This study not only enhances the understanding of the nonlinear dynamic process of dissipative soliton generation, but also offers a novel approach for designing ultrafast lasers characterized by high stability and an all-fiber structure.

Keywords: mode-locked fiber laser, thulium-doped fiber, pulsed laser, dissipative soliton

PACS: 42.55.Wd, 42.65.Tg, 42.60.–v, 42.65.Re

DOI: 10.1088/1674-1056/ae063c **CSTR:** 32038.14.CPB.ae063c

1. Introduction

Mode-locked fiber lasers have been intensively researched and applied in various fields, including materials processing, soliton dynamics, optical sensing, and ultrafast spectroscopy, owning to their significant advantages of high peak powers, ultrashort pulse widths, and good optical system compatibility.[1–4] Generally, these high-performance pulsed lasers are implemented by using mode-locking technology that is mainly divided into two categories: active mode-locking and passive mode-locking. Active mode-locking usually adopts electro-optical modulators (EOM) or acousto-optic modulators (AOM),[5,6] which achieve pulse shaping by periodically altering the amplitude or phase of the optical field within the cavity through external signals. However, active mode-locking systems are complex, and the introduction of additional modulation devices may adversely affect the laser's overall performance. In contrast, passive mode-locking using real saturable absorbers (SAs) based on nonlinear optical absorption effects, offers obvious strengths of robustness, simple system structure and narrower pulse width.

Up to now, real SAs based on different materials for mode-locking have been successfully demonstrated, which include graphene,[7] semiconductor saturable absorber mirror (SESAM),[8] carbon nanotube (CNT),[9] black phosphorus (BP),[10] chalcogenide,[11] topological insulators (TIs),[12] and tellurium-containing compounds,[13,14] among others.[15] However, these materials often have certain limitations in practical applications. Graphene is typically weak in light absorption, and has a low damage threshold. SESAMs are usually designed for a specific wavelength range, and the fabrication process is relatively complex. Carbon nanotubes are poorly dispersed and prone to agglomeration. Black phosphorus is chemically unstable and susceptible to oxidation in air. Chalcocite, TIs and tellurium-containing compounds generally need to be produced using chemical vapor deposition, photo-induced deposition or magnetron sputtering technology, which make the fabrication complicated and laborious. Meanwhile, SAs based on fiber doped with rare metal ions, e.g., holmium, thulium, gallium, have attracted considerable attention and become a hot research topic, due to its inherent strengths such as insensitivity to perturbations in fiber cavities, high damage threshold, long lifetime, and excellent flexibility.[16–18]

In 2003, Tordella demonstrated the first pulsed laser based on doped fiber-SA. In the neodymium-doped fiber laser, a chromium-doped fiber was employed as the saturable absorber, and laser pulses operating at 1084 nm were achieved.[19] Subsequently, Tsao *et al.* used thulium-doped fiber as the saturable absorber to realize *Q*-switched operation at 1570-nm wavelength in an erbium-doped fiber laser.

†Corresponding author. E-mail: yangkun@zzuli.edu.cn

© 2026 Chinese Physical Society and IOP Publishing Ltd. All rights, including for text and data mining, AI training, and similar technologies, are reserved.

The obtained 1570-nm laser source served as a pump source to pump the thulium-doped fiber, which simultaneously functioned both as gain medium and SA. Ultimately, ultrashort pulses with a pulse width of 720 ps at 1950 nm were generated.[20] Later, Lau *et al.* employed an erbium-ytterbium-thulium co-doped fiber for mode locking, in their experiments, both dark solitons and bright solitons operating in the 1.5-μm band were observed.[21] Then, Zhang *et al.* utilized a bismuth-doped fiber as the mode-locker in an erbium-doped fiber laser, in which stable triple-wavelength vector dark solitons with 335-ns pulse width were produced.[22] Recently, Kirsch *et al.* presented an 1877-nm fiber laser using a thulium-doped fiber for mode-locking operation, where bright soliton pulses with 600-fs duration and 1 nJ energy were realized.[23] To date, most research of pulsed laser schemes based on doped fiber saturable absorbers have focused on the anomalous dispersion region, where conventional solitons (CSs) are initiated through the interplay between group velocity dispersion (GVD) and self-phase modulation (SPM). Notably, according to the soliton area theorem determination, the energy of a single CS pulse is inherently limited.[24] In comparisons, dissipative solitons (DSs) generated in net-normal-dispersion or/and in all-normal-dispersion region can achieve relatively high pulse energies, where nonlinearity, dispersion, gain, and loss within the cavity need to accomplish in a multifaceted balance.[25] Therefore, exploring the use of doped fiber-SAs to generate dissipative solitons in normal dispersion lasers provides fascinating possibilities.

In this paper, we experimentally demonstrate an Er-doped fiber laser operating in net normal dispersion region, where a Tm-doped fiber function as a mode-locker. By precisely manipulating the pump power and intracavity polarization state, stabilized individual dissipative soliton pulses are obtained. Moreover, with the gradual increase of the pump power, the spectral morphology undergoes a parabolic shape, Π-shape, and M-shape. The cavity gain and the fiber birefringence possess great influence on the emergence. By increasing the gain, multiple dissipative pulses including soliton pairs and triples are induced because of the peak power clamping effect. This laser exhibits the peculiarities of all-fiber configuration, high stability and excellent tenability, which can provide new insights for the optimized design of ultrafast lasers.

2. Experimental setup

The experimental schematic of the constructed mode-locked fiber laser is demonstrated in Fig. 1. A 980-nm laser diode with a maximum output power of 500 mW is used to pump a 2.6-m long erbium-doped fiber (EDF) via a 980 nm/1550 nm wavelength division multiplexer (WDM). Providing gain within the cavity, the EDF features a GVD parameter of −26 (ps/km)/nm at 1550 nm and an absorption coefficient of 80 dB/m at 1530 nm. A polarization-independent isolator (ISO) is inserted to ensure unidirectional light propagation within the cavity. Additionally, a thulium-doped fiber (TDF, Nufern, SM-TSF-9/125) with a length of 12 cm is employed as a saturable absorber for achieving mode-locking operation. A three-plate polarization controller (PC) is enabled to adjust the polarization state and loss within the cavity, thereby shaping and optimizing the laser pulses. A 90:10 optical coupler (OC) is also incorporate into the cavity, where 90% of the light sustains oscillation within the resonator and 10% of the optical signal is output for detection. All optical components in the system are connected by standard single-mode fiber (SMF-28) tails, with a GVD of 17 (ps/km)/nm at 1550 nm. The total length of the SMFs inside the cavity is 2.81 m, and the overall length of the cavity is around 5.53 m. Ignoring the dispersion generated by optical components and the shorter TDF, the net dispersion within the cavity is calculated to be 0.025 ps^2.

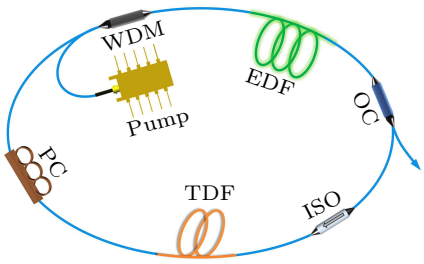


Fig. 1. Schematic diagram of the dissipative soliton laser system. WDM: wavelength-division multiplexer; EDF: erbium-doped fiber; TDF: thulium-doped fiber; PC: polarization controller; SMF: single-mode fiber; ISO: polarization-insensitive isolator; OC: optical coupler.

Since the fiber laser operates in the net- normal dispersion regime, dissipative soliton pulses are enabled under the multiple balance between gain and loss, nonlinearity and dispersion, spectral filtering, and saturable absorption effects.[26] The output pulse spectra were precisely measured using an optical spectrum analyzer (Yokogawa AQ6370D) with a resolution of 0.02 nm. The temporal and frequency characteristics of the laser pulses were monitored and analyzed by an oscilloscope (Rohde & Schwarz, RTO 2022, 2 GHz) and a spectrum analyzer (Keysight N9000B), respectively, equipped with a high-speed photodetector (Newport 818BB-51F) with a bandwidth of 10 GHz to convert the optical signals into electrical signals.

3. Results and discussion

In the experiment, when the pump power exceeded 180 mW, stable dissipative soliton pulses were observed by careful adjusting the polarization controller. The output pulses characteristics are depicted in Fig. 2. As shown in Fig. 2(a), the output spectral edges exhibit a steep distribution, coinciding well with the generic feature of nonlinear pulse propagation in normal dispersion fiber lasers. Notably, different from

the typical DSs with rectangular shapes, the optical spectrum displays a bell-like shape with a narrow spectrum width. The central wavelength of the dissipative soliton is 1565.88 nm, featuring a 3-dB bandwidth of 1.20 nm, similar to the characteristics observed in the SESAM pulsed laser,[27] which is attributed to the narrow bandwidth spectral filtering effect induced by limited gain bandwidth.[28] Besides, this spectral feature may also originate from significant birefringence or/and birefringence filtering effects within the cavity.[29] Figure 2(b) presents the time-domain signal trace of the pulse on the oscilloscope, exhibiting a pulse period of 27.1 ns, coinciding with the cavity length of 5.53 m. The inset in Fig. 2(b) illustrates the pulse's time-domain characteristics over a wider temporal range of 32 μs, where no noticeable temporal jitter is appeared, indicating the good stability. Due to the lack of autocorrelation device in the laboratory, a magnified monopulse profile of the dissipative soliton is demonstrated to characterize the pulse width. As depicted in Fig. 2(c), the full width at half maximum (FWHM) is ∼ 1.07 ns, by fitting with a Gaussian function. Actually, the real pulse duration would be considerably shorter if an autocorrelator were used to evaluate its pulse width. Figure 2(d) presents the radio-frequency (RF) spectrum of the pulse. The fundamental frequency rate is 36.9 MHz at a 2-kHz resolution, and the signal-to-noise ratio is 64 dB. The inset in Fig. 2(d) illustrates the frequency-domain signal over a broader range of 400 MHz, with no modulated signals appearance, further conforming excellent stability of the dissipative soliton operation. In the meanwhile, the laser output power transmitted via the 10% output port is approximately 16.24 mW, resulting in a peak power of around 0.41 W. This combination of broad pulse width and low peak power renders such a simple DS laser system an ideal candidate for seed pulse generation in amplification applications.

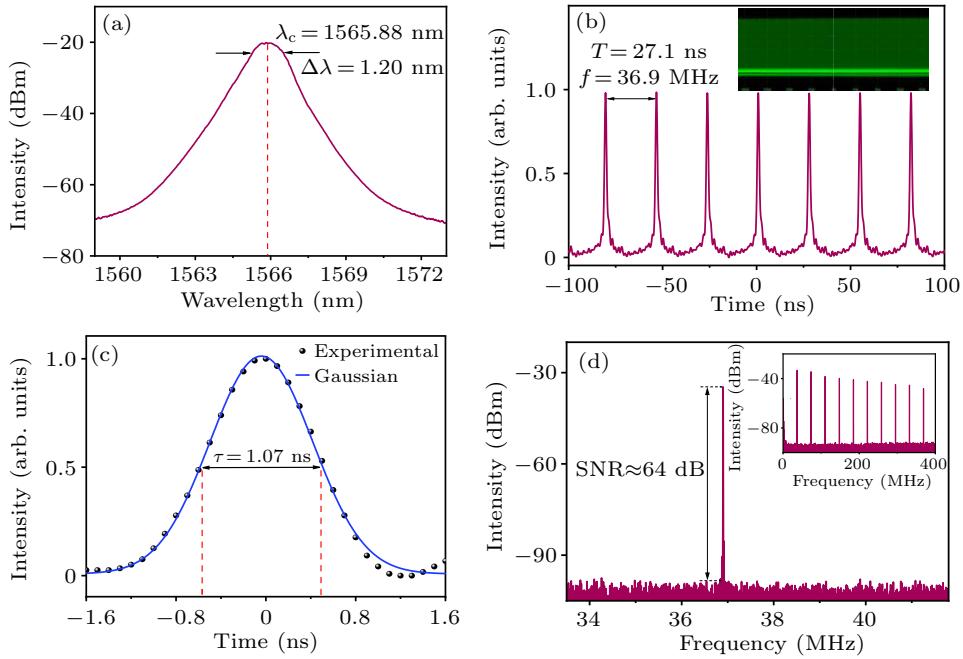


Fig. 2. Pulse characteristics at the pump power of 180 mW: (a) mode-locked spectrum, (b) temporal pulse train, (c) single pulse signal, and (d) radio frequency spectrum.

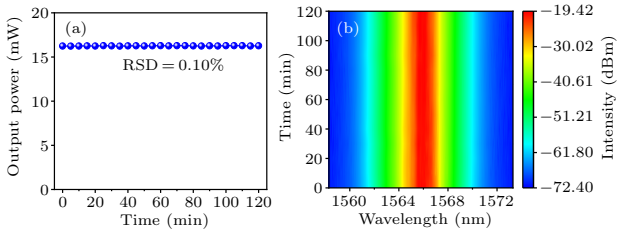


Fig. 3. Stability test results of the laser: (a) output power variation and (b) spectral changes.

Considering that stability is a crucial factor for evaluating the applicability in practical systems, we placed the laser in a controlled laboratory environment without external interference, and monitored the variation of the corresponding output power and optical spectra at five-minute intervals over a period of two hours. As shown in Fig. 3(a), the average output power remains consistent throughout the recording process, with a relative standard deviation (RSD) of 0.1%. Figure 3(b) illustrates the spectrum evolution, displaying no significant changes. The measured data above confirm that the usability of the pulsed laser is robust.

Particularly, we noted that the spectral profiles of the single DS pulse undergoes a dynamic change at varying pumping levels. As shown in Figs. 4(a) and 4(b), when the pump power increased from 240 mW to 280 mW, the spectrum was transformed from a parabolic to a Π-shaped morphology, with the spectrum shifting from 1565.96 nm to 1566.12 nm. Meanwhile, the 3-dB spectral bandwidths were raised from 1.39 nm to 1.55 nm. Compared with the spectrum of 180 mW in Fig. 2(a), it can be observed that the central wavelength of

the spectrum was redshifted and the 3-dB bandwidth gradually changed in an escalating trend. This phenomenon is originated from that the self-phase modulation (SPM) of the pulse is significantly enhanced as the pump power increases.[30,31] Peculiarly, when the pump power was elevated to 310 mW, as exhibited in Fig. 4(c), the spectrum became M-shaped, and two prominent spectral lobes emerged with the spectrum centers located at 1565.86 nm and 1566.70 nm, and the 3-dB bandwidths of 0.35 nm and 0.33 nm, respectively. Remarkably, it should be mentioned that the center wavelength can also be relocated by adjusting the PC; however, in the process described above, we did not modify the direction of the polarization controller. Therefore, the appearance of the M-shaped spectrum induced by the increased pump power can be attributed to the enhanced absorption processes in the erbium-doped fiber, leading to a decrease in gain at the center of the spectrum, while higher gain can still be obtained on both sides, so the cavity filtering effects was enhanced and obvious peaks on both sides are formed.[31] In addition, the mode competition may potentially further induce this phenomenon. Figure 4(d) provides the corresponding pulse shapes variation of the dissipative solitons at different pump powers. Due to the increase in pumping power, the thulium-doped fiber's saturable absorption effect is enhanced, leading to a decrease in the cavity pulse width from 936 ps to 839 ps.

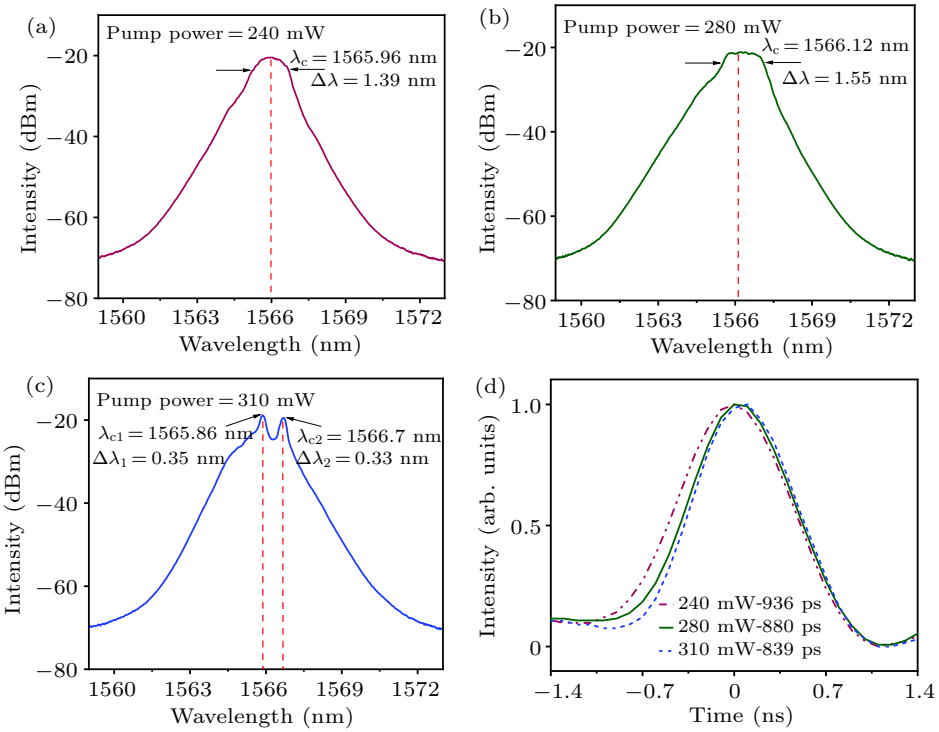


Fig. 4. The comparative results of the generated DS under different pump power: (a)–(c) optical spectrum evolution, (d) variation of pulse shape.

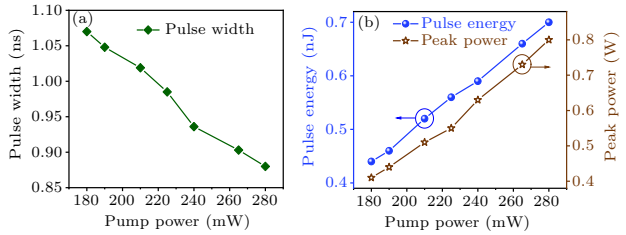


Fig. 5. Output pulse duration, pulse energy and peak power versus pump power.

In addition, we also analyzed the relationships among output pulse duration, pulse energy, peak pulse power and pump power. As depicted in Fig. 5, increasing the pump power from 180 mW to 280 mW results in a decrease of pulse duration from approximately 1.07 ns to 0.88 ns, while the output pulse energy and the peak pulse power experience slight increase from 0.44 nJ to 0.7 nJ, and from 0.41 W to 0.8 W, respectively. This variation trends can be primarily ascribed to the nonlinear absorption characteristics of the TDF-saturable absorber, meaning that an increase in pulse intensity correlates with an increase in transmittance.

As described above, stable single dissipative soliton operation can be facilitated in a limited pump power range. When the pumping intensity dramatically changed beyond this range, the balance required for the formation of single-soliton states was broken, then multi-soliton states were occurred.[31] As shown in Figs. 6(a), 6(b), and 6(c), fundamental dissipative pulses were observed when the power was between 180 mW and 320 mW; dissipative soliton pairs were appeared between 320 mW and 460 mW; and dissipative soliton triplets were emerged under the pump power range from 460 mW to 500 mW. The corresponding periods are 27.1 ns, 13.7 ns, and

9.0 ns, respectively. We also measured the corresponding RF spectrum signals. As depicted in Figs. 6(d), 6(e), and 6(f), the frequency rates are 36.9 MHz, 73.0 MHz, and 111.1 MHz, respectively. Noteworthy, the SNR of the different soliton states all exceed 60 dB, which further illustrates that this dissipative soliton laser possess good stability. Notably, these multiple pulses are uniformly distributed, and their spacing can be adjusted by changing the gain distribution within the cavity. For the formation of the multiple dissipative solitons, it is contributed to peak-power-clamping effect.[32] That is, further increases in pump strength do not contribute to the amplification of the soliton itself; instead, they enhance the background dispersive waves. Rather than forming a noise-like wave, the background dispersive waves are rapidly transformed into a new DS, which subsequently gives rise to the emergence of multiple dissipative solitons. Under certain conditions, these multiple pulses can equalize via a self-arrangement process and finally form an orderly distributed pulse sequence with uniform spacing.

In addition to having good stability, the obvious advantage of this laser is the construct with all-fiber structure, benefiting for optical system compatibility. Table 1 summarizes the performance of some mode-locked lasers using different SAs. In comparison, this proposed laser using TDF-SA exhibits almost comparable performances in terms of operating wavelength, pump power threshold, and repetition frequency. By further optimizing the system, such a simple and compact pulsed laser could potentially be leveraged in those applications such as ultrafast optical communication and photonic integration.

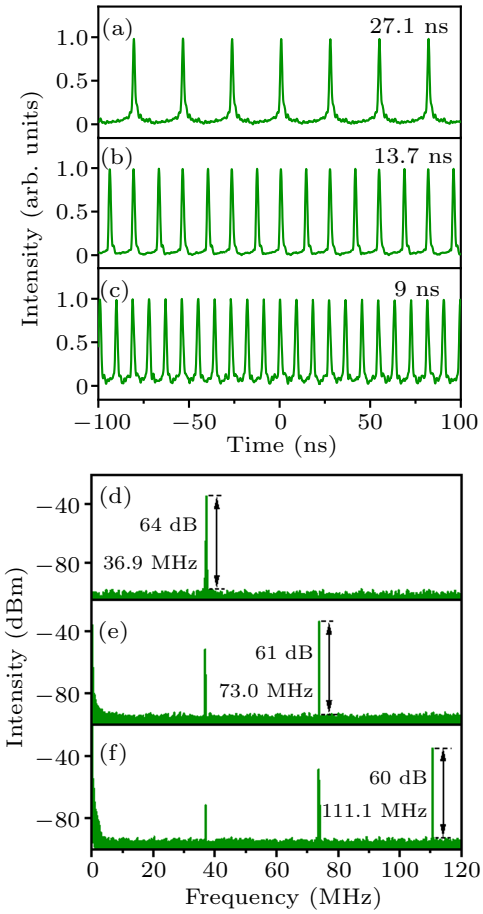


Fig. 6. Multi-soliton states under different pump levels: (a)–(c) temporal signals, (d)–(f) the corresponding RF spectrum signals.

Table 1. Mode-locked fiber lasers using different SAs.

Pulsed laser	SA materials	Pump threshold (mW)	Wavelength (nm)	Frequency rate (MHz)	SNR (dB)	Ref.
EDF	TDF	180	1565.88	36.9	64	this work
EDF	graphene	22.6	1556.1	9.1	61	[7]
YDF	SESAM	70	1030	10.96	70	[8]
YDF	BP	258.6	1067.1	0.39	64.9	[10]
EDF	GeS_2	600	1568	7.49	71	[11]
EDF	Sb_2Te_3	90	1558	25.38	68	[12]
EDF	Bi_2O_2Te	60	1559.44	7.48	67.25	[13]
EDF	PbTe	–	1569.9	6.25	54.2	[14]
EDF	ULPG	50	1535.3	2.09	–	[15]

4. Conclusion

In conclusion, a passively mode-locked fiber laser utilizing a TDF-saturable absorber and operating in the net normal dispersion regime has been experimentally demonstrated. By meticulously adjusting the polarization state within the cavity, stable dissipative solitons are manifested. The generated fundamental DS exhibits a center wavelength of 1565.88 nm, a 3 dB bandwidth of 1.2 nm, a repetition rate of 35.17 MHz, and an SNR of 64 dB. As the pump power is increased, the spectral profiles of individual solitons are varied, assuming either a parabolic-like, Π-like, or M-like shape. Correspondingly, the pulse duration decreases slightly, from approximately 1.07 ns to 0.84 ns. Moreover, further increasing the pump power results in the emergence of dissipative soliton pairs and triples, originating from the pulse peak clamping effect within the cavity. This laser with an all-fiber structure is compact and highly stable, which may offer great potential applications in optical communication and optical sensing.

Acknowledgements

Project supported by the National Natural Science Foundation of China (Grant Nos. 62105296 and 62305209), the Key Research and Development Projects of Henan Province, China (Grant No. 241111212600), the Henan Provincial Science and Technology Research Project (Grant Nos. 252102220036 and 242102210145), the Key Research Project of Higher Education Institutions of Henan Province, China (Grant No. 26A510020), and the Youth Backbone Project of Zhengzhou University of Light Industry.

References

[1] Fermann M E and Hartl I 2013 *Nat. Photon.* **7** 868
[2] Zhang W, Zhan L, Xian T and Gao L 2019 *Opt. Lett.* **44** 4008
[3] Li X H, Huang X W, Hu X C, Guo X X and Han Y H 2023 *Opt. Laser Technol.* **158** 108898
[4] Zhang C, Wu T, He S, Zhang C and Fu B 2024 *Opt. Laser Technol.* **168** 109865
[5] Huang J, Lan X, Wei T, Han Q, Gao Z, Zhou Z and Xiao H 2012 *Opt. Lett.* **37** 494
[6] Cuadrado-Laborde C, Bello-Jiménez M, Díez A, Cruz J L and Andrés M V 2014 *Opt. Lett.* **39** 68
[7] Lau K Y, Abu Bakar M H, Muhammad F D, Latif A A, Omar M F, Yusoff Z and Mahdi M A 2018 *Opt. Express* **26** 12790
[8] Zou F, Wang Z K, Wang Z W, Bai Y, Li Q and Zhou J 2017 *Opt. Laser Technol.* **92** 133
[9] Huang L, Zhang Y and Liu X 2020 *Nanophotonics* **9** 2731
[10] Wang T, Zhang W, Wang J, Wu J, Hou T, Ma P, Su R, Ma Y, Peng J, Zhan L, Zhang K and Zhou P 2020 *Opt. Laser Technol.* **123** 105948
[11] Kan X F, Yang Z X, Liu B, Li S Y, Ye G J, Xie Z Y, Luo Y L, Liu X Y, Lu Y, Zhang Y, Zhang J R, Shen Z, Xu J, Su W, Yin C, Yu Q, Zhu S C and Wu J 2024 *ACS Appl. Nano Mater.* **7** 7989
[12] Boguslawski J, Sobon G, Zybala R and Sotor J 2015 *Opt. Lett.* **40** 2786
[13] Hui Z Q, Bu X F, Wang Y H, Han D D, Gong J M, Li L, Li X H and Yan S Y 2022 *Adv. Opt. Mater.* **10** 2201812
[14] Li X H, Xu W S, Wang Y M, Zhang X L, Hui Z Q, Zhang H, Wageh S, Al-Hartomy O A and Al-Sehemi A G 2022 *Appl. Mater. Today* **28** 101546
[15] Guo B, Guo X, Tang L, Yang W, Chen Q and Ren Z 2021 *Chin. Opt. Lett.* **19** 071405
[16] Gene J, Kim S K and Lim S D 2018 *J. Lightwave Technol.* **36** 2183
[17] Lau K Y, Yasin S Z M, Ker P J, Mansor A, Abdul-Rashid H A, Kamil Y M and Mahdi M A 2019 *Opt. Laser Technol.* **119** 105615
[18] Al-Alimi A W, Yusoff N M, Cholan N A, Alresheedi M T, Abas A F, Talib Z A and Mahdi M A 2022 *Results in Phys.* **33** 105167
[19] Tordella L, Djellout H, Dussardier B, Saissy A and Monnom G 2003 *Electron. Lett.* **39** 1307
[20] Tsao H, Chang C, Lin S, Sheu J and Tsai T 2014 *Opt. Laser Technol* **56** 354
[21] Lau K Y, Yusoff N M, Abdul Hadi M A W, Abas A F, Alresheedi M T and Mahdi M A 2020 *Opt. Laser Technol.* **124** 105937
[22] Zhang P, Nizamani B, Najm M M, Dimyati K, Yasin M and Harun S W 2021 *Opt. Lett.* **46** 3336
[23] Kirsch D C, Bednyakova A, Varak P, Honzatko P, Cadier B, Robin T, Fotiadi A, Peterka P and Chernysheva M 2022 *Commun. Phys.* **5** 219
[24] Tang D Y, Zhao L M, Zhao B and Liu A Q 2005 *Phys. Rev. A* **72** 043816
[25] Renninger W H, Chong A and Wise F W 2008 *Phys. Rev. A* **77** 023814
[26] Li D, Tang D, Zhao L and Shen D 2015 *J. Lightwave Technol.* **33** 3781
[27] Yang N, Huang C, Tang Y and Xu J 2015 *Laser Phys. Lett.* **12** 055101
[28] Ma X, Zhang Y, Lin J, Dai C, Xu L, and Yao P 2024 *Laser Technol.* **48** 153
[29] Peng J, Sorokina M, and Zeng H 2021 *J. Light. Technol.* **39** 6579
[30] Yan D, Li X, Zhang S, Han M, Han H and Yang Z 2016 *Opt. Express* **24** 739
[31] Abdelalim M A, Logvin Y, Khalil D A and Anis H 2009 *Opt. Express* **17** 2264
[32] Li J, Wang C and Wang P 2022 *J. Lightwave Technol.* **40** 5958